
**CCUS: 4183120**

# Time-Lapse Monitoring of CO2 Sequestration: 1D Visco-elastic Waveform Inversion Applied to Distributed Acoustic Sensing-Acquired Zero offset Vertical Seismic Profile – a Feasibility Study

Yu Chen, Takashi Mizuno, Joël Le Calvez, SLB



## Abstract

Automated processing is required for long-term monitoring of carbon storage. This study is the first to investigate the feasibility of using Distributed Acoustic Sensing (DAS)-acquired zero-offset vertical seismic profile (ZOVSP) also referred to ZOVSP DAS and 1D viscoelastic waveform inversion for automated monitoring of carbon sequestration operation. We estimate the uncertainty of automated solution quantitatively using field data and conclude that our method reliably detects velocity reductions associated to carbon sequestration operation. Additionally, we highlight the need for high signal-to-noise ratio (SNR) data to effectively resolve changes in attenuation.

## Introduction

Time-lapse monitoring of carbon sequestration operations is essential to ensure the safe and effective storage of $CO_2$ in geological formations. Different seismic methods have been developed for long-term monitoring of $CO_2$ plume migration (e.g., Egorov et al., 2017). However, it is critical to develop cost-effective solutions for long-term operations. In the last decade, Distributed Acoustic Sensing (DAS) emerges as a cost-effective solution for vertical seismic profiling to monitor $CO_2$ injection and storage. Automated processing is another key for long-term monitoring.

We developed a cost-effective acquisition system and an effective 1D viscoelastic waveform inversion scheme. This study evaluates the feasibility and value of leveraging waveform inversion technology for automated monitoring solutions. This method is applicable for long-term automated monitoring solutions since the method inverts parameters without human intervention.

## Method

We developed a viscoelastic waveform inversion (VWI) method (Chen et al., 2021). The method employs viscoelastic ray-based waveform modeling (Leaney et al., 2019). This algorithm handles 3D survey geometry while the velocity model is 1D. It computes the rays between the two points and convolves with a specific source wavelet input.

We employ an optimization method of downhill simplex (Press et al., 2007) to invert the compressional velocity (*Vp*), the compressional attenuation (1/*Qp*), and source amplitude. To avoid strong coupling among *Vp*, *Qp* and source amplitude, we separate *Vp* from *Qp* and source amplitude inversion. We also use different objective functions for inversion of *Vp* and the inversion of *Qp* to make the inversion robust. The objective function of the *Vp* inversion is a combination of time residuals and L2 norms of waveforms. The time residual term ensures a fast convergency like tomography, and the L2 norm enables the inversion to fit the entire waveform.

To invert *Qp* and source amplitude, we employ a combination of L2 norm of the maximum amplitudes and the maximum correlation coefficient (CC) of each trace as the objective function. The maximum CC can capture the source duration, and the amplitudes contain the information of amplitude decay. *Vp* and *Qp* are updated iteratively until the waveform fitting reaches the criterion (Chen et al., 2021; Chen et al., 2022).

## Data

The cost and environment footprint were minimized while ensuring the project's objectives were achieved. We performed the zero-offset vertical seismic profile (ZOVSP) acquisition using a wireline-deployed DAS and a portable seismic source. The small explosive is loaded inside the cartridge and buried just beneath the surface. The explosive is triggered manually, and it generates mainly P-wave (Figure 1). The direct P-wave is clearly seen to a depth of about 6,000 ft below the surface using a single shot. The amplitude varied with each shot within 20 % of peak-to-peak amplitude, and the shape of the wavelet is comparable although certain variations were observed. Time intervals between shots were about a few minutes therefore we should not expect any variation in subsurface velocity and Q structure. The variation between each waveform could be considered as variation in shot signature including coupling of source at near surface.

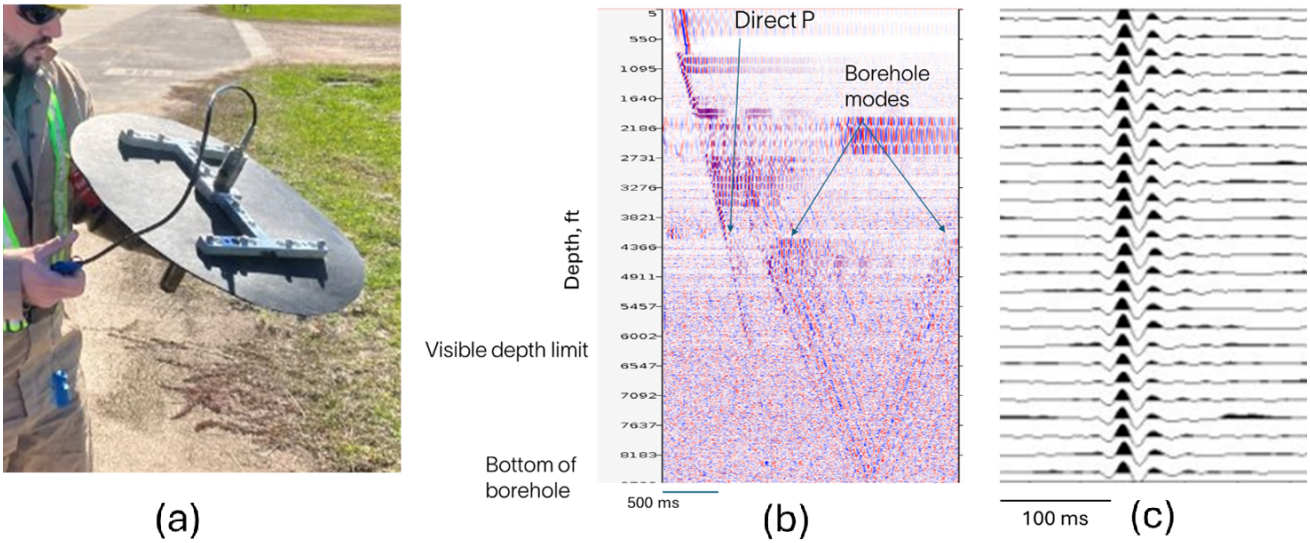


Figure 1: (a) Overview of the handy seismic source used in the study. (b) Example of DAS-acquired waveforms. Due to variations inside the well, we have seen coupling issues in several section of the borehole. In the present study, we focused on the depth section where the coupling is adequate. We applied a 5 – 50 Hz bandpass filter. (c) Detail view of the onset of the P wave among all 26 shots used in the present study.

## Results

The experiment resulted in the acquisition of 30 shot gathers, with acceptable data quality for 26 shots. We applied the VWI method to the data recorded between 360 and 484 meters deep to evaluate the repeatability of *Vp* and *Qp* extraction leveraging the VWI approach for different shots.

For the first inversion, the initial *Vp* model is built from scratch, with a layer above the top receiver and 8 layers in the receiver depth (~15 m thick). The Q model has two layers with a layer above the top receiver and the other in the receiver's depth range. We do not have any prior information of the models. The inversion obtains a model which produce the synthetics to best fit the data. Figure 2a show the fitting between the data (black) and synthetics (red) for the first shot. After we obtain the inverted model for the first shot, the inverted model is used as the initial model for the rest of the inversion. The inversion of each shot takes approximately 5 minutes. Users need to change the input data only.

The *Vp* inversion results of 26 shots (Figure 1b) are consistent with each other, with a standard deviation ($\sigma_{Vp}$) of ~2% (Figure 1c). Previous studies suggest that $CO_2$ injection can reduce *Vp* by 5–10%, and the consistency of our results supports the combination of DAS VSP and VWI is feasible to detect changes for $CO_2$ injection automatically. However, *Qp* values showed more scatter, with $\sigma_{Qp}$ of ~ 100% (Figure 1d). While rock physics models suggest that *Qp* can decrease to around 50 during $CO_2$ injection, we are not confident that our method can resolve *Qp* changes associated with $CO_2$ injection.

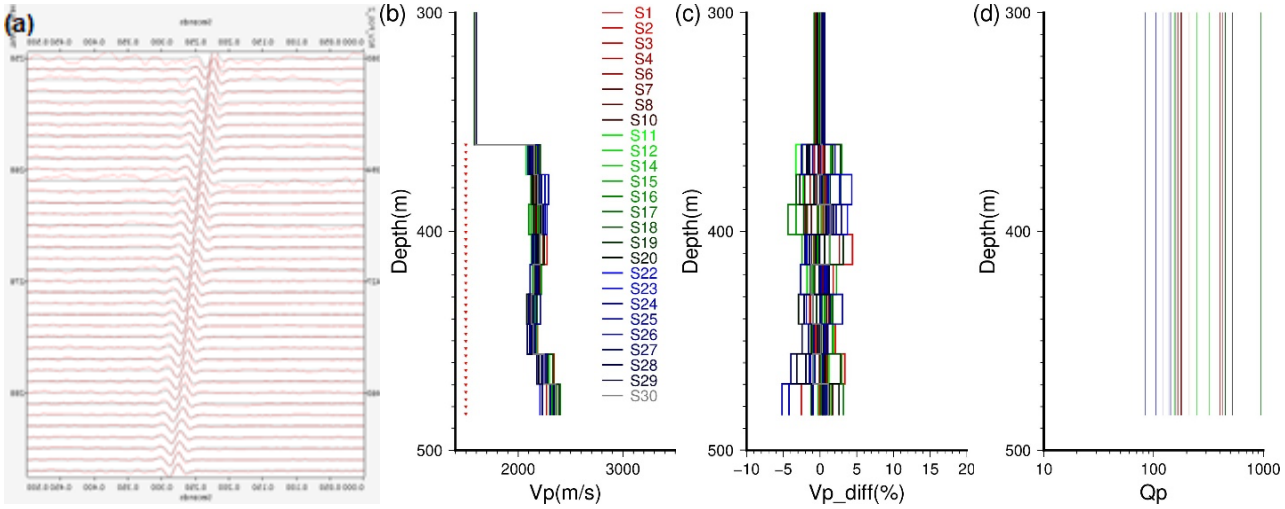


Figure 2: (a) Waveform fitting of the data (black) and the synthetics (red) for the first shot. (b) Inverted velocity models with the data of the 26 shots. Red inverse triangle represents the receivers. (c) Inverted velocity difference from the average with the 26 shots in (b). (d) Inverted Q models with the 26 shots.

## Discussion

We observed a big uncertainty in terms of *Qp* inversion in the data tested, owing to the low signal-to-noise ratio (SNR) of 4 in the datasets acquired. The *Qp* inversion is not as sensitive as the *Vp* inversion, because *Vp* variation can cause arrival time differences and waveform distortion, while *Qp* variations cause much less waveform distortion. The noise would distort the waveforms and cause uncertainty in the *Qp* inversion.

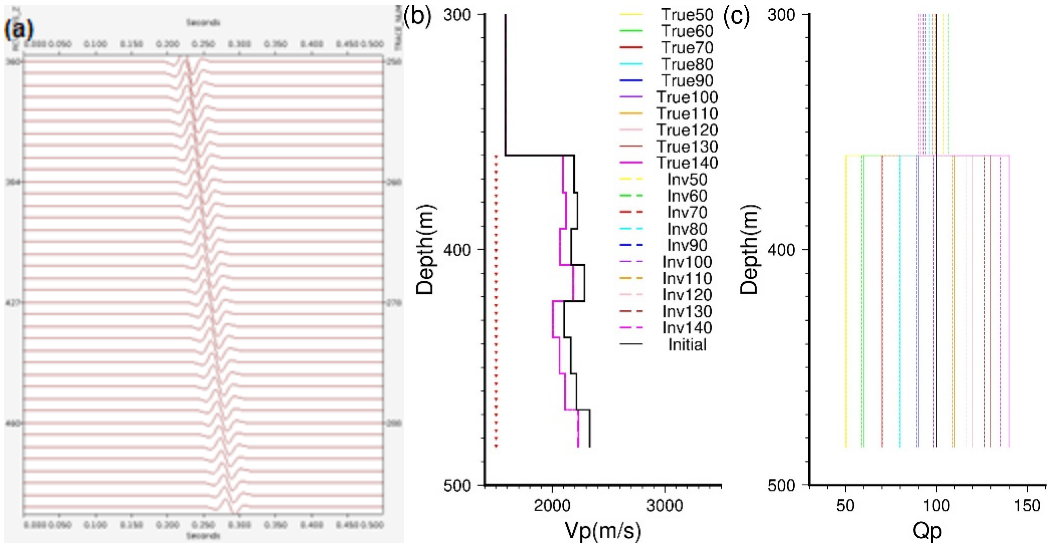


Figure 3: (a) Waveform fitting of the data (black) of a synthetic shot and the synthetics (red). (b) Inverted *Qp* models of the 10 synthetic shots with the *Qp* value from 50 to 140 (with an interval of 10). Different colors represent diffferent *Qp* models. Color sold curves represent the true models while color dashed curves represents the inverted model. The black sold curve is the initial model.

We conducted synthetic tests with varying noise levels to examine the impact of noise on *Qp* inversion. We performed inversions of noise-free data of the 10 shots. Compared to Figure 2a, the synthetics waveforms fit the data well (Figure 3a). Once the waveform fitting is good, we are able to resolve the *Qp* with a much higher resolution. The inverted *Qp* models (colored dashed curves) are consistent with the true *Qp* model (colored solid curve). All the *Vp* models are identical to the purple model by visual inspection. The $\sigma_{Qp}$ is less than 1% (Figure 3b). The inverted *Vp* models are almost identical to the true models.

We add and increase the gaussian noise to test the robustness of *Vp* and *Qp* inversion. With a SNR of 10, the $\sigma_{Vp}$ is less than 1%, and the $\sigma_{Qp}$ increased to 20%. Therefore, the inversion can still resolve time-lapse *Qp* variation owing to $CO_2$ injection. In data with a SNR of 4, matching the real data's noise level, the inversion cannot fully match the data (Figure 4a). The $\sigma_{Vp}$ and $\sigma_{Qp}$ rise to 2% and 75%, respectively. This suggests that noise plays a major role in the scattering of *Qp* values, though other factors may also contribute. The results demonstrate that better quality data is required to better resolve the *Qp* model. Either better acquisition system or waveform stacking might improve the data quality.

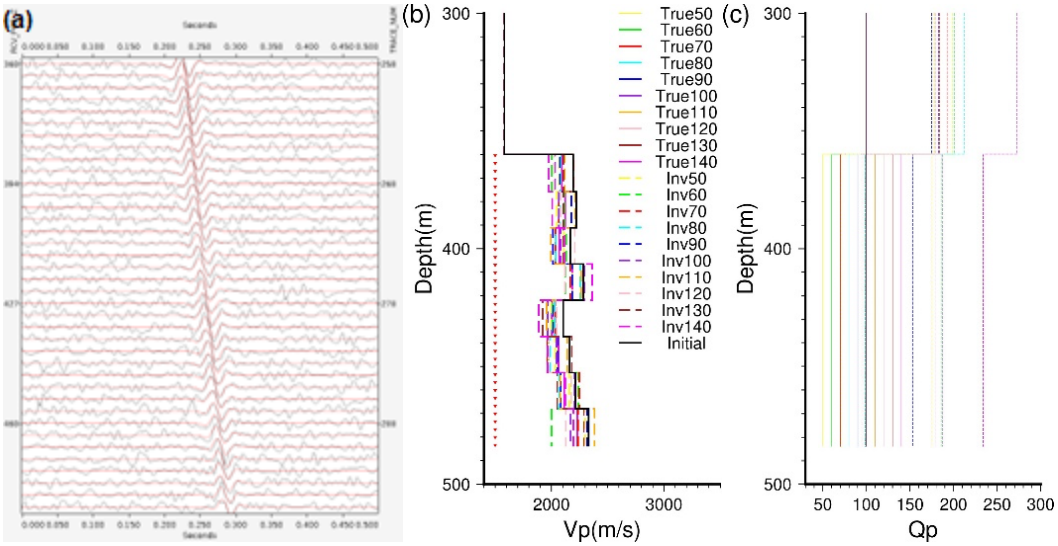


Figure 4. (a) Waveform fitting of the noisy data (black) with a SNR of 4 and the synthetics (red). (b) Inverted velocity models with the synthteic data of 10 synthetics shots. (c) Inverted Q models of the 10 shots. Different colors represent diffferent *Qp* models. Color sold curves represent the true models while color dashed curves represents the inverted model. The black sold curve is the initial model.

## Conclusions

This study uses a newly developed viscoelastic waveform inversion and a DAS-acquired ZOVSP dataset to study the feasibility of automated monitoring of carbon sequestration operation. We demonstrate that time-lapse of P-wave velocity reductions associated with carbon sequestration operation can be detected. However, the changes in *Qp* may not be captured when the SNR is not high enough. Synthetic tests demonstrate that *Qp* can be resolved effectively with high SNR data.

We present a simple workflow for automated monitoring leveraging a short computational time while only input data is required, no manual processing is needed. This method is applicable for long-term automated monitoring solutions since the method inverts parameters without human intervention.

## References

Chen, Y., T. Mizuno, P. Bettinelli, J. Le Calvez, 2021. 1D viscoelastic waveform inversion of zero-offset vertical seismic profile data. First International Meeting for Applied Geoscience & Energy, 3515-3519.

Chen, Y., S. Ali, Mizuno, P. Bettinelli, J. Le Calvez, 2022. The importance of viscoelastic waveform inversion in VSP: Synthetic studies. Second International Meeting for Applied Geoscience & Energy, 3614-3618.

Egorov, A., R. Pevzner, A. Bóna, S. Glubokovskikh, V. Puzyrev, K. Tertyshnikov, and B. Gurevich, 2017. Time-lapse full waveform inversion of vertical seismic profile data: Workflow and application to the CO2CRC Otway project, Geophys. Res. Lett., 44, 7211–7218, doi:10.1002/2017GL074122.

Leaney, S., T. Mizuno, E. Velez, T. Cuny, and M. Perez, 2019. Integrated anisotropic model building, DAS simulation and imaging. 89th Annual meeting, SEG Expanded Abstracts, 999-1003.